Engineering Science and Technology, an International Journal 20 (2017) 629–636

HOSTED BY

Contents lists available at ScienceDirect

Engineering Science and Technology, an International Journal

journal homepage: www.elsevier.com/locate/jestch

Full Length Article

A survey on OFDM channel estimation techniques based on denoising strategies

Pallaviram Sure [a,*], Chandra Mohan Bhuma [b]

[a] Dept. of Electronics & Communication Engineering, M S Ramaiah University of Applied Sciences, India
[b] Dept. of Electronics & Communication Engineering, Bapatla Engineering College, India

ARTICLE INFO

Article history:
Received 25 May 2016
Revised 22 August 2016
Accepted 15 September 2016
Available online 23 February 2017

Keywords:
Pilot aided channel estimator
MMSE techniques
LS techniques
Denoising threshold
OFDM
MIMO–OFDM

ABSTRACT

Channel estimation forms the heart of any orthogonal frequency division multiplexing (OFDM) based wireless communication receiver. Frequency domain pilot aided channel estimation techniques are either least squares (LS) based or minimum mean square error (MMSE) based. LS based techniques are computationally less complex. Unlike MMSE ones, they do not require a priori knowledge of channel statistics (KCS). However, the mean square error (MSE) performance of the channel estimator incorporating MMSE based techniques is better compared to that obtained with the incorporation of LS based techniques. To enhance the MSE performance using LS based techniques, a variety of denoising strategies have been developed in the literature, which are applied on the LS estimated channel impulse response (CIR). The advantage of denoising threshold based LS techniques is that, they do not require KCS but still render near optimal MMSE performance similar to MMSE based techniques. In this paper, a detailed survey on various existing denoising strategies, with a comparative discussion of these strategies is presented.

1. Introduction

The current wireless communication standards are progressing towards 5G [1]. Further, energy efficiency is a major concern in many applications including wireless communications. For example energy aware clustering protocols are developed for heterogenous wireless sensor networks in [2]. Further, an investigation on energy efficient sensor node placement in railway station for monitoring railway tracks and rail tunnels is presented in [3]. Energy efficiency is also one of the challenges in 5G communication systems. Such systems can be realized by incorporating multi input multi output OFDM (MIMO–OFDM) technology. MIMO–OFDM promises higher energy and spectral efficiencies, while mitigating inter symbol interference (ISI) [4]. Starting with 3G, the wireless communications standards have incorporated OFDM technology, to reduce the inter symbol interference, obtain higher data rates and better system spectral efficiency. The heart of any OFDM receiver is the channel estimation block. Efficiency of the channel estimation has a direct impact on the bit error rate (BER) performance of the OFDM system. This paper considers data aided (pilot aided) channel estimation in frequency domain.

Frequency domain channel estimation techniques employ known symbols called pilots at known positions in the OFDM symbol grid. These pilots are arranged in a regular manner as comb-type, block-type [5] or 2D-grid type [6]. In a comb-type arrangement, the pilots are present in few subcarriers of all OFDM symbols, while in block-type arrangement, the pilots are present in few OFDM symbols on all subcarriers. In 2D-grid type arrangement, the pilots are present in few subcarriers of few OFDM symbols. Thus the number of pilots in 2D-grid type is less than that in comb-type or block-type arrangements. However, reliability in terms of system BER is better for comb-type arrangement in fast fading channel environments [5]. At the receiver, the channel is estimated using known and the received pilot symbols. Frequency domain channel estimation techniques are either LS based, MMSE based or maximum likelihood (ML) based ones. In this paper, LS and MMSE techniques have been primarily considered.

The MMSE based techniques utilize second order KCS and render near optimal performance than the LS based techniques [5]. However, they suffer from the drawbacks of higher computational complexity and the practical unavailability of second order channel statistics. The LS based frequency domain channel estimation methods are simple to implement and do not require any KCS. To improve the MSE performance of the LS based channel estimator, many denoising threshold based strategies have been developed in the literature. This enhances the MSE performance of the

* Corresponding author.
E-mail address: pallaviram.sure@yahoo.com (P. Sure).
Peer review under responsibility of Karabuk University.

http://dx.doi.org/10.1016/j.jestch.2016.09.011
2215-0986/

channel estimator and in turn improves the BER performance of the receiver, which is at par with the MMSE based techniques. The denoising techniques require KCS parameters like channel length, number of channel taps, and AWGN noise power, which are not easily estimated in practice.

For estimating a frequency selective Rayleigh fading channel in OFDM systems, an EM-based iterative algorithm is developed in [7]. The EM algorithm is a methodology to find maximum likelihood estimates of system required parameters in problems where observed data are incomplete. The algorithm provides an initial estimate of CIR with the help of pilot symbols. This initial CIR estimate is iterated using an E-step and a Q-step, to obtain the final CIR. The algorithm achieves a near-optimal CIR estimate within few iterations. Another low complexity EM algorithm is developed in [8], and a sparse Bayesian learning (SBL) technique is employed in [9], to estimate the channel and its second order statistics jointly. As, this paper focusses on LS and MMSE techniques, the ML techniques have not been further discussed.

The rest of the paper is organized as follows. The baseband model for a typical OFDM system is introduced in Section 2. Subsequently, available options for various blocks in OFDM system are also discussed. In Section 3, a detailed survey on the available denoising strategies is presented. Pilot aided channel estimation in MIMO–OFDM systems is briefly addressed in Section 4. The paper concludes in Section 5.

2. OFDM system model

The baseband model for a typical OFDM wireless communication system, is shown in Fig. 1. The binary data to be transmitted, is first mapped using digital modulation schemes like binary phase shift keying (BPSK), quadrature phase shift keying (QPSK) or quadrature amplitude modulation (QAM). The modulated data symbols are converted from serial to parallel form. One column of data symbols forms a single OFDM symbol. Multiple OFDM symbols form the OFDM grid. Each row of data symbols is termed as subcarrier. If one OFDM symbol comprises of N data symbols, the number of subcarriers are N. The pilot insertion block is used to transmit known data, which is optional. Pilots are known data symbols, which assist in estimating the channel at the receiver. Each OFDM symbol is converted to time domain using an inverse DFT (IDFT) operation. A cyclic prefix (CP) is attached at the beginning of each time domain OFDM symbol to counteract the distortion caused by ISI in the channel. CP is the replica of last part of any given OFDM symbol. Instead of CP, a Zero Padding (ZP) can also be used. However, CP is more effective than ZP in combating ISI [10]. After the insertion of CP, the resultant OFDM symbols are converted to serial form and are transmitted through a wireless channel.

The channel may be of flat fading type or frequency selective fading type. In any case, at the receiver, the presence of additive white Gaussian noise (AWGN) is inherent. In this paper, perfect synchronization is assumed between the transmitter and receiver. Imperfect timing or frequency synchronization causes reduced BER performance of any given channel estimation technique. In practice, timing synchronization can be achieved by exploiting the structure of CP [11].

At the receiver, the received symbols are converted to parallel form and the CP is removed. The resulting OFDM symbols are sent through a DFT block and the corresponding frequency domain symbols are obtained. A pilot based equalizer uses these symbols to estimate the channel and further processes the received data to estimate transmitted OFDM symbols. There symbols are then converted to serial form and are demapped, to obtain the transmitted binary data.

Equalizer: It comprises of a channel estimator and a symbol estimator. An LS based channel estimator is shown in Fig. 2. Using retrieved and known pilot symbols, an LS estimation is performed at the pilot positions. The LS estimated channel frequency response (CFR) is interpolated to obtain CFR at all positions (data and pilot). It is then converted to CIR using an IDFT block, which is denoised by performing truncation and thresholding operations. Subsequently the denoised CFR is obtained. The symbol estimator is a one tap equalizer, which uses the estimated channel frequency response (CFR) and the received symbols to estimate the transmitted symbols.

In general, at the receiver, the ith received OFDM symbol, notated as $Y_{i,k}$ is given in (1), where $H_{i,k}$ is the CFR, $X_{i,k}$ is the transmitted OFDM symbol and $N_{i,k}$ is the AWGN in the ith symbol duration. The range of subcarrier index k is $[0, N-1]$, where N represents the total number of subcarriers. The expression in (1) assumes that inter carrier interference (ICI) is negligible [5].

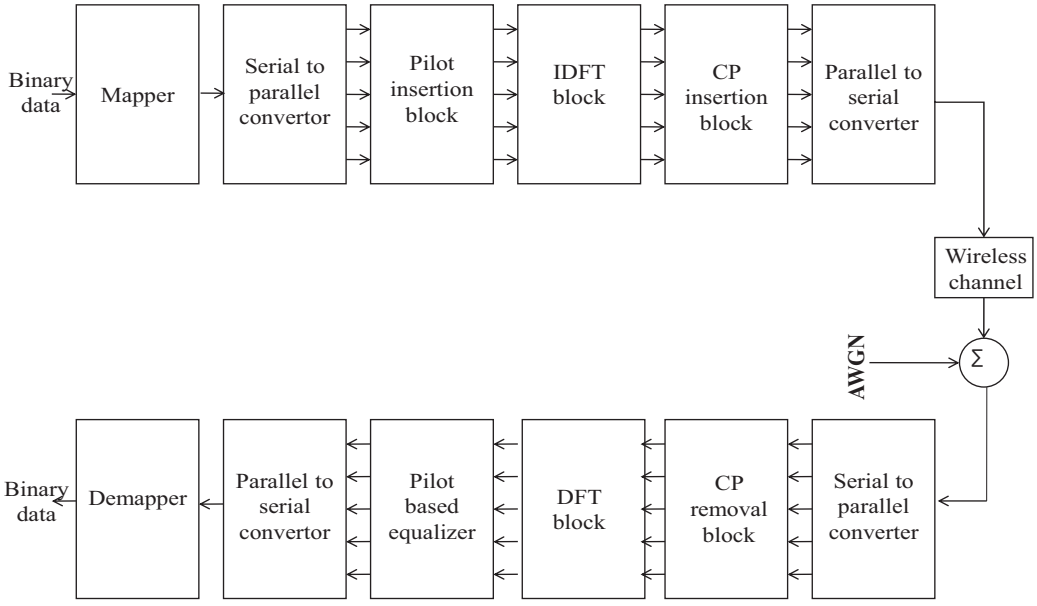

Fig. 1. A typical baseband OFDM system.

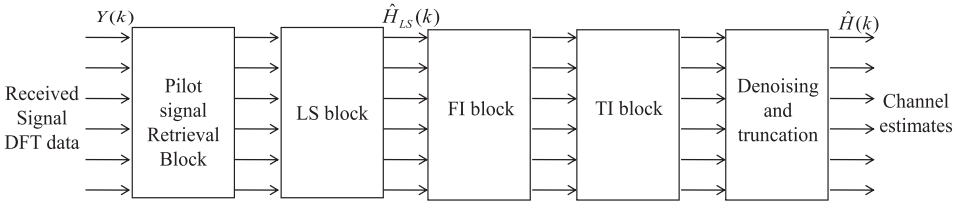

Fig. 2. Pilot-aided channel estimator.

$$Y_{i,k} = H_{i,k}X_{i,k} + N_{i,k}, \quad 0 \leqslant k \leqslant N-1 \tag{1}$$

The channel estimator at the receiver processes $Y_{i,k}$ as shown in Fig. 2. The pilot positions in each OFDM symbol, represented as $P(k)$ and transmitted pilot symbols, say, $X_{i,k}, k \in P(k)$, are already known at the receiver. The LS block estimates the channel frequency response (CFR) coefficients as in (2).

$$H_{i,k}^{LS} = \frac{Y_{i,k}}{X_{i,k}}, \quad k \in P(k) \tag{2}$$

To obtain the CFR at all subcarrier positions, interpolation techniques are used. The interpolated CFR is $H_{i,k}^{LS}, 0 \leqslant k \leqslant N-1$. Then substituting for $Y_{i,k}$ in $H_{i,k}^{LS}$, using (1), the LS estimated CFR can be expressed as in (3). In (3), $V_{i,k} = \frac{N_{i,k}}{X_{i,k}}$. Taking IDFT on this CFR, CIR estimates are obtained as in (4).

$$H_{i,k}^{LS} = H_{i,k} + V_{i,k}, \quad k \in [0, N-1] \tag{3}$$

$$h_{i,n}^{LS} = h_{i,n} + v_{i,n}, \quad 0 \leqslant n \leqslant N-1 \tag{4}$$

In (4), $h_{i,n}$ is the actual CIR corrupted by complex gaussian noise $v_{i,n}$. Assuming L as channel length, the estimated CIR after $n = L-1$ is forced to zero, called as truncated CIR, given by (5). Applying denoising threshold represented as ϑ on (5), the denoised CIR is finally given by (6). Available interpolations and denoising strategies are discussed in the forthcoming sections.

$$\hat{h}_{i,n} = \begin{cases} h_{i,n}^{LS} & 0 \leqslant n \leqslant L-1 \\ 0 & L \leqslant n \leqslant N-1 \end{cases} \tag{5}$$

$$\hat{h}_{i,n}^{t} = \begin{cases} \hat{h}_{i,n}, & \left|\hat{h}_{i,n}\right|^2 > \vartheta \\ 0, & otherwise \end{cases} \tag{6}$$

2.1. Interpolator designs for channel estimation

As seen from Fig. 2, interpolator is an essential block for channel estimation. If comb-type pilots are employed, the LS estimated CFR obtained at the pilot subcarrier positions, must be interpolated in the frequency direction (subcarrier direction), to obtain the CFR coefficients at non pilot positions. This helps in obtaining $H_{i,k}^{LS}$ of (2) at all subcarrier positions, which further helps in obtaining the CIR, $h_{i,n}^{LS}$ in (4). Some of the interpolation techniques are linear, second order, cubic or a spline interpolator [5]. In a linear interpolation, given two adjacent CFR coefficients, the CFR coefficients in between them are obtained assuming a straight line nature between the two given ones. In a second order or cubic interpolation, a second order curve and a cubic curve are assumed between the given two adjacent CFR coefficients. The higher the order of interpolation, the better is the channel estimation [5]. Polynomial interpolation, which outperforms the cubic interpolation, has been explored in [12,13], which are generalised versions of n_{th} order interpolation.

Other than the above ones, DFT and IDFT based interpolations have also been investigated in [14–16]. In a DFT based interpolation, the given CFR coefficients are first transformed using DFT or IDFT, which are zero padded. Then using IDFT or DFT respectively, the CFR are reconstructed. The length of reconstructed CFR sequence is longer than the original CFR sequence before interpolation. The IDFT based interpolation, referred as time domain interpolation outperforms the linear and second order interpolations, but is inferior to spline interpolation as shown in [5]. The DFT based interpolation outperforms the IDFT based interpolation as shown in [17]. Further, the DFT based interpolation is shown to be much better than linear, second order, cubic, time domain and the low pass interpolations in [18].

If block-type pilot arrangements are used, interpolation is required in time direction (symbol direction). Frequency interpolators can be employed as time interpolators. If 2D-grid type of pilot arrangements are used, interpolation has to be carried out in both time and frequency directions. Time domain interpolators are explored in [19,6,20,21]. Interpolation can be performed simultaneously in time and frequency, which are explored in [22,23].

3. Denoising strategies for channel estimation

To improve the MSE performance of the LS based techniques to approach that of the MMSE techniques, a powerful tool is denoising. Denoising is the process of eliminating noise from a noisy signal. The LS estimated and interpolated CFR given in (3) and corresponding CIR in (4) can be observed to be corrupted by noise. Hence, the CIR in 4 can be treated as a noisy signal, and can be denoised to obtain a better CIR estimate. Denoising can be performed by pruning the CIR coefficients using a threshold.

The threshold can be devised in time domain or in any other transformed domain like frequency, wavelet and eigen. However, denoising operation is performed on the LS estimated and interpolated CIR, which is in time domain. Thresholding strategies are often derived by employing optimization criteria. A threshold distinguishes significant channel impulse response (CIR) taps from the noisy taps. Segregation of significant CIR taps from the noisy CIR taps, becomes a tap-detection problem, for which many solutions are available in the existing literature, discussed as follows.

The LS estimated CIR is truncated assuming known channel length, without employing a threshold [24]. In this process, the CIR taps below the channel length are all considered as significant taps, while the CIR taps after the channel length are considered noisy and are truncated to zero. Compared with a no truncation case, truncation of CIR taps improved the MSE performance of the channel estimator [24]. For channel estimation in OFDM systems, intra-symbol time domain averaging approaches are devised [25]. Assuming known channel length, according to the method, the significant CIR taps are selected based on a threshold, which is a fraction of known maximum channel tap's energy. This method is called as most significant tap (MST) selection method. It is shown to be better than that of truncation of CIR scheme as in [24]. However, it should be noted that, KCS information in the form

of channel length and maximum channel tap energy are necessary for this denoising scheme.

Two different strategies for MST selection are presented in [25]. The first strategy incorporates fixed number of signal taps, while the second strategy chooses all the significant taps above a specified threshold, ϑ. OFDM system simulations show that a good choice of the threshold is within (20–23) dB lower to the operating $\frac{1}{SNR}$. The BER performance of this method is shown to be better than the conventional method of truncation.

Iterative channel estimation techniques have been popularized in LTE systems, which are considered in [26,27]. An iterative channel estimation algorithm applicable for OFDM systems, in the presence of sparse channels is devised in [28]. This algorithm incorporates the LS technique along with a generalized Akaike information criterion (GAIC), to simultaneously obtain the estimates of channel length and also the significant CIR tap positions. Using system simulations, the method has been demonstrated in [28] for its better MSE performance compared to the method of [24]. The algorithm proceeds by defining GAIC as given in (7), where V_L represents the error term obtained, while modeling the channel to length L and the second term corresponds to the penalty. γ is fixed as 2, though it can take any value in $1.5 \leqslant \gamma \leqslant 2.5$. The error term V_L is given in (8), where $\hat{\sigma}^2_{n,L}$ represents the estimate of time domain noise variance calculated with a channel length L.

$$GAIC(L) = V_L + \gamma ln(ln(N))(L+1) \tag{7}$$

$$V_L = \frac{N}{2} ln\left(\hat{\sigma}^2_{n,L}\right) \tag{8}$$

The channel estimation algorithm initially assumes $P = L_{cp}$, where L_{cp} is the assumed channel length. For each $L \in [1, P]$, the GAIC value is computed. Then the channel length is estimated as $\hat{L}$, given in (9). Further to find out the significant channel tap positions, it is assumed that $P = \hat{L} - 1$. The procedure of GAIC computation is repeated to compute new value of $\hat{L}$ given in (9). This procedure is repeated till $L = 1$. Then the list of all $\hat{L}$ obtained from the GAIC minimization correspond to the tap positions. The algorithm is also shown as a block diagram representation in Fig. 3. Simulations show that this algorithm renders better MSE performance than the method of truncation used in [24].

$$\hat{L} = \arg\min_L GAIC(L) \tag{9}$$

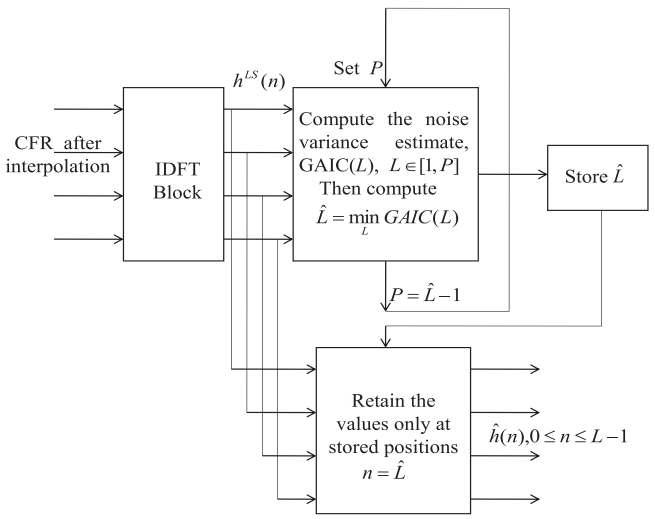

Fig. 3. GAIC minimization based channel estimation.

Assuming known channel length, a threshold is derived from the MSE expression, using an optimality condition in [29]. Derived threshold is equal to twice the noise power in time domain. The time domain noise power is easily estimated by averaging the noise-only part of the LS estimated CIR, assuming known channel length. The computer simulations demonstrated the fact that the devised algorithm performs better in terms of MSE and system BER compared to that in [24]. The threshold expression is given as in (10).By changing the threshold from $0.5\sigma_v^2$ to $5\sigma_v^2$, the MSE plots for a given SNR have been obtained in the study of [29]. The results show that the MSE is better when the threshold $\vartheta = 2\sigma_v^2$.

$$\sigma_v^2 = \frac{1}{N-L}\sum_{n=L}^{N-1}\left|h^{LS}(n)\right|^2 \tag{10}$$

Assuming a sparse channel, a threshold is developed in [30], by maximizing the probability of correct detection. By pruning the LS estimated CIR with the derived threshold, an improved CIR estimate is obtained. Compared to the MST method [25] and the GAIC method [28], this method showed better MSE performance. However, incorporation of the derived threshold requires the knowledge of the complete power profile, noise variance and also channel length. The threshold expression is shown in (11), where γ_n^2 represents the channel power at nth CIR coefficient position. The knowledge of channel power profile implies $\gamma_n^2,\ n \in [0, N-1]$ is required a priori, which is impractical.

$$\vartheta = \sigma_v^2 \ln\left(2 + \frac{\gamma_n^2}{\sigma_v^2}\right) \tag{11}$$

A threshold is devised using wavelet domain, which is the standard deviation of the noise obtained from wavelet decomposition, in [31,32]. Using OFDM system simulations, it is observed that the wavelet based threshold performs much better than the threshold in [29]. The threshold expression is given in (12), where d_i is the detail component obtained by the wavelet decomposition of the LS estimated CIR.

$$\vartheta = \left(\frac{median|D|}{0.6745}\right)^2 \tag{12}$$

A suboptimal threshold is derived by minimization of MSE expression framed by incorporating the probability of false alarm and probability of correct detection in [33]. The derived threshold demands a priori knowledge of many channel parameters. To overcome this, a threshold is framed by fixing the overall false alarm probability of the tap detection. The correspondingly obtained threshold expression is given in (13). Here, N_p represents the number of pilot subcarriers, ρN_p is the inverse of time domain noise variance, and $\bar{P}_{ofa}$ is the probability of false alarm. The results showed that by sacrificing $\bar{P}_{ofa}$, the MSE performance improved and is better that in [29,30].

$$\vartheta = \frac{\ln\left(\bar{P}_{ofa}\right)}{\rho N_p} \tag{13}$$

An optimal threshold is developed based on MSE minimization in [34]. The MSE is formulated using the events namely, tap excision, tap holding, noise excision and noise holding. The threshold derived requires channel length, number of significant channel taps (N_t) and the noise variance a priori. As these actual values are not known in practice, the threshold tends to be suboptimal. The threshold expression is given in (14).

$$\vartheta = \frac{\ln\left(\frac{(N_p - N_t)\rho N_p}{N_t^2}\right)}{\rho N_p - N_t} \tag{14}$$

Energy based MST selection strategies have also been presented in [34]. An instantaneous energy selection (IES) scheme is devised, where, the channel taps are accumulated such that the sum of instantaneous energies of all the taps put together reaches a target T. This is shown in (15). Here, $h_{x,y}$ implies CIR of yth OFDM symbol in the xth subcarrier, N_p represents number of pilot subcarriers, which are chosen to be more than the channel length L. This scheme is shown to perform better than many other existing thresholding strategies.

Another energy based strategy devised in [34] is the average energy selection (AES) scheme, shown in (16). Here, $\hat{E}_{il}$ represents the combined energy in the CIR samples of W consecutive OFDM symbols in the ith subcarrier, which is given in (17) and ς represents the threshold. Both these schemes render better MSE performance than when these are not utilized with a given threshold expression. Also AES is observed to perform better than IES, as the window length W increases. But this implies more storage is required.

$$S_{IES}(l) = \left\{ i(j) : \sum_{v=0}^{j-1} \left| h^{LS}_{i(v),l} \right|^2 \leqslant T,\ j = [0, N_p - 1] \right\} \tag{15}$$

$$S_{AES}(l) = \left\{ i : \hat{E}_{il} > \varsigma,\ i = [0, N_p - 1] \right\} \tag{16}$$

$$\hat{E}_{il} = \frac{1}{W} \sum_{v=l-W+1}^{l} \left| h^{LS}_{i,v} \right|^2 \tag{17}$$

A universal threshold based channel estimation algorithm is developed for sparse channels in [35]. This threshold is estimated from the noise coefficients of the LS estimated CIR. The algorithm is shown to achieve better MSE and BER performances with moderate complexity, compared to that of [29]. The universal threshold is given in (18), where L_{cp} is the assumed length of the channel. σ_n^2 is the variance of noise at nth CIR coefficient position. The standard deviation of noise is estimated using (19).

$$\vartheta = 2L_{cp}\sigma_n^2 \tag{18}$$

$$\hat{\sigma}_n^1 = \sqrt{2}\sigma = \frac{\sqrt{2}\,median\left|h^{LS}\right|}{\sqrt{\ln 4}} \tag{19}$$

A block diagram representation of the universal threshold based denoising strategy is shown in Fig. 4 [35]. Here $\hat{\sigma}_n^{11}$ is the standard deviation of noise obtained in step 3 of the algorithm. The final CIR is notated as $\hat{h}$, for $n \in [0, L_{cp} - 1]$. The simulation results showed that the universal threshold based channel estimation method performed better than those in [29,25].

The denoising strategies discussed in this section are summarized in Table 1. Though the optimal thresholds render near MMSE performance to the channel estimator, there are few practical issues which hinder their MSE performance. The optimal threshold expressions comprise of KCS parameters like L, N_t and σ_v^2. which should be consistently estimated in practice. Errors due to KCS estimation cause unavoidable MSE degradation. This is characterized analytically in [36]. Further, to overcome MSE degradation, an eigen-select threshold has been developed, which is shown in (20). In (20), f is the function of eigen values, $\lambda_{\min}$ and $\lambda_{\max}$ are the minimum and maximum eigen values of the estimated autocorrelation matrix of the LS estimated and interpolated CIR. The eigen-select threshold does not use any KCS estimation, but reduces MSE degradation. It is shown to outperform the thresholds proposed in [29–31,34,35]. However, the computational complexity of this method is more than that of the others compared.

$$\vartheta = f(\lambda_{thr}),\ \lambda_{\min} \leqslant \lambda_{thr} \leqslant \lambda_{\max} \tag{20}$$

A weighted-noise threshold is proposed, which balances the MSE degradation due to KCS estimation in [37],. The corresponding proposed threshold is given in (21, where the parameter q can be estimated by a procedure proposed in [37]. The work showed that for a good estimate of q, the weighted-noise threshold based channel estimation outperforms the other thresholds proposed in [29–31,34–36].

$$\vartheta = (q+1)\sigma_v^2 \ln\left(\frac{(q+2)}{(q+1)} + \frac{1}{(q+1)\sigma_v^2 N_t}\right) \tag{21}$$

4. Channel estimation in MIMO–OFDM systems

In contrast to OFDM, in a MIMO–OFDM system multiple transmitters and multiple receivers exist. Hence, pilot aided channel estimation is a high dimensional problem in MIMO–OFDM and massive MIMO–OFDM systems. In a $N_t \times N_r$ MIMO–OFDM system, a total of $N_t N_r$ channels have to be estimated at the receiver. The type of pilot symbols used and their positions should be selected such that, the receiver can distinguish all the $N_t N_r$ estimated channels. In this section, some of the available pilot strategies for MIMO–OFDM systems have been addressed. In addition to denoising based channel estimation, the symbol detection problem is also discussed.

4.1. Pilot strategies

For MIMO–OFDM systems, the comb-type, block-type and 2D-grid type pilot arrangements can be extended to be used at multiple transmitters. This requires the additional incorporation of nulls (no transmissions). Conventionally, comb-type pilot arrangements are used for MIMO–OFDM systems. Consider the case of a two antenna system. First subcarrier of first antenna carries pilots, at all positions. Similarly second subcarrier of second antenna carries

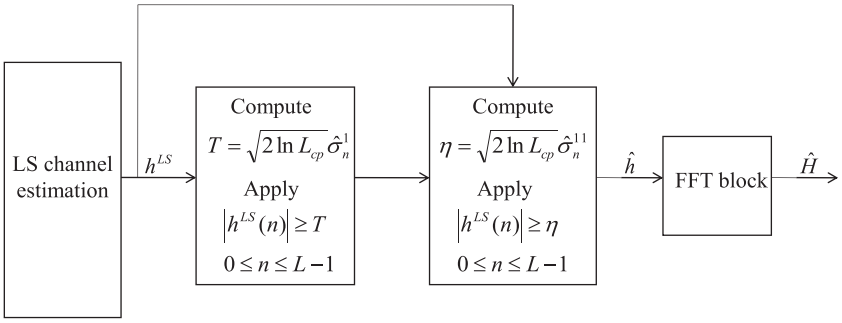

Fig. 4. Channel estimation using universal threshold.

Table 1
Summary of denoising thresholds.

Article	Threshold	KCS Parameters			BER performance
		L	N_t	σ_v^2	
[24]	Truncation	Yes	No	No	Better than no threshold
[25]	20–23 dB of $\frac{1}{SNR}$	No	No	Yes	Better than no threshold
[28]	Iterative Scheme	No	No	No	Better than [24]
[29]	$2\sigma_v^2$	Yes	No	Yes	Better than [24]
[30]	$\sigma_v^2 \ln\left(2+\frac{1}{N_t\sigma_v^2}\right)$	No	Yes	Yes	Better than [25,28]
[31]	$\left(\frac{median\lvert D\rvert}{0.6745}\right)^2$	Yes	No	No	Better than [29]
[33]	$\frac{\ln\left(N_p/P_{ofa}\right)}{\rho N_p}$	Yes	No	No	Better than [29,30]
[34]	$\frac{\ln\left(\frac{(N_p-N_t)}{N_t^2\sigma_v^2}\right)}{\left(\frac{1}{\sigma_v^2}-N_t\right)}, N_p > L$	Yes	Yes	Yes	Better than [29,30,33]
[35]	$2\sigma_v^2 \ln(L)$	Yes	No	Yes	Better than [29]
[36]	$f(\lambda_{thr}),\ \lambda_{\min} \leqslant \lambda_{thr} \leqslant \lambda_{\max}$	No	No	No	Better than [29] to [35]
[37]	$(q+1)\sigma_v^2 \ln\left(\frac{(q+2)}{(q+1)}+\frac{1}{(q+1)\sigma_v^2 N_t}\right)$	No	No	No	Better than [29] to [36]

pilots at all positions. In the first subcarrier of second antenna, and second subcarrier of first antenna, only nulls are transmitted. This type of comb-type arrangements are studied for 2×2 MIMO–OFDM systems in [38]. However, as the system configuration increases to more than 2 antennas, the amount of overhead, in the form of both nulls and pilots increases.

One method to overcome the above said problem, is to employ Chu sequences with a block-type pilot arrangement. Such a channel estimation strategy is devised for MIMO–OFDM systems in [39], whose performance is shown to be better than that of a conventional comb-type MIMO–OFDM system, while reducing the required pilot overhead. In [39], for a 4×4 MIMO–OFDM system, each pilot OFDM symbol of a single transmit antenna, is loaded with a unique Chu sequence. At each transmit antenna, the Chu sequence is a phase shifted version of the corresponding Chu sequence at the remaining transmit antennas. Chu sequences have nearly ideal auto-correlation and cross-correlation properties. Exploring this property at each receive antenna, the unknown MIMO–OFDM channels are estimated using a DFT based method, without using interpolation at all. The channel estimation is performed in time domain unlike the conventional comb-type system, where channel estimation is carried out in frequency domain. This technique exploits the fact that, delay in time domain reflects as phase shift in frequency domain. Thus pilots are embedded in frequency domain, while channel estimation is carried out in time domain. A special time–frequency training scheme has been devised in [40] for MIMO–OFDM systems, where pilots are spread both in time domain as well as in frequency domain, but the occupied overhead is still small.

4.2. Channel estimation and symbol detection

For a OFDM system with comb-type overhead, let the transmit sequence in frequency domain be $X_{q,i}(k), 0 \leqslant k \leqslant N_t - 1$ for ith OFDM symbol of qth transmitter. Set of sub-carriers $\{k\}$, employed to carry pilots are not the same for all the transmit antennas. For qth antenna, the subcarrier index k is $\{q, q+S_f, q+2S_f, \ldots\}$, where S_f represents pilot sub-carrier spacing. Observe that, on a single sub-carrier, if qth antenna transmits pilots, rest of the antennas transmit nulls on that sub-carrier, as shown in Fig. 5.

Using the received symbols and known pilot symbols, at known positions, channel estimation is carried out at each receive antenna. First, the CFR is estimated at pilot positions using LS method. Then the obtained CFR is interpolated in each OFDM symbol to obtain the CFR coefficients at all data, pilot and null positions, which implies CFR at all the N subcarrier positions.

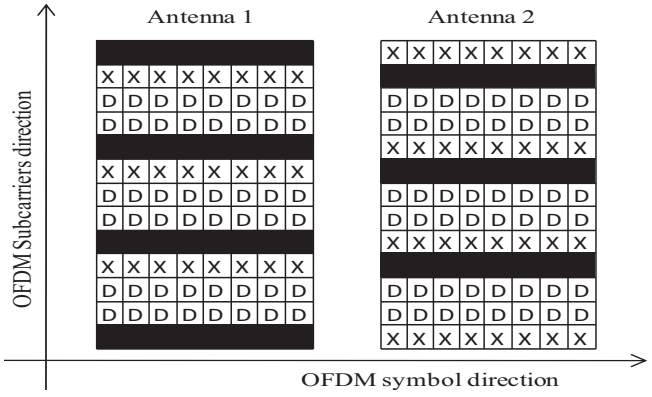

Fig. 5. CTCP overhead arrangement for 2×2 MIMO–OFDM system.

Let the ith OFDM symbol received at pth antenna be given as (22), where $X_{a,i}^D$ is the diagonal matrix formed by the entries of $X_{a,i}$. The LS channel estimates before and after interpolation are given in (23), and (24) respectively, where, $\hat{H}_{pq,i}$ is estimated CFR between qth transmit and pth receive antenna on ith OFDM symbol. Corresponding CIR is notated as $\hat{h}_{pq,i}$.

$$Y_{p,i} = \sum_{a=1}^{N_{tx}} H_{pa,i} X_{a,i}^D + W_{p,i} \tag{22}$$

where, $0 \leqslant p \leqslant N_{rx} - 1$

$$\hat{H}_{pq,i}(k) = \frac{Y_{p,i}(k)}{X_{q,i}(k)}, \quad k \in \{q, q+S_f, q+2S_f, \ldots\} \tag{23}$$

$$\hat{H}_{pq,i}(k) = \frac{Y_{p,i}(k)}{X_{q,i}(k)}, \quad 0 \leqslant k \leqslant N-1 \tag{24}$$

Note that for MIMO channel estimation, the pilots are arranged such that when the one of the transmit antenna is sending pilots, the other antennas transmit nulls. So all $X_{a,i}$ are nulls except $X_{q,i}$, which is the pilot sequence. Therefore (22) can be reduced to (25), which is a single input single output (SISO) representation between mth receive antenna and nth transmit antenna.

$$Y_{p,i} = H_{pq,i} X_{q,i}^D + W_{p,i} \tag{25}$$

$$\hat{h}_{pq,i}(n) = h_{pq,i}(n) + v_{p,i}(n), \quad 0 \leqslant n \leqslant N-1 \tag{26}$$

Substituting (25) in (24), time domain version of (24) is given by (26). Here, $v_{p,i}(k)$ represents modulated noise term. Thus, according to the second term of (26), it is seen that the estimated CIR, $\hat{h}_{pq,i}$ is noisy. As discussed in Section 3, the denoising strategies can be employed on the CIR of (26) and the corresponding CFR is provided to the symbol detector.

Performance of channel estimation techniques for SISO–OFDM systems can be studied using MSE vs. SNR and BER vs. SNR plots. It should be noted that BER is obtained after the received data is finally decoded as binary data. In the case of a MIMO–OFDM system, design of such a decoder is also a high dimensional problem. An optimal decoder would be maximum likelihood detector or maximum aposteriori (MAP) detector. However, such a decoder cannot be implemented as the configuration of MIMO system grows massive [41]. Therefore for massive MIMO–OFDM systems, one category of algorithms are based on local neighborhood searching strategies. Some such algorithms are the likelihood ascent search (LAS) [42] and reactive tabu search (RTS) [43]. Another category of algorithms approach near-MAP performance, some of which are belief propagation (BP) algorithm [41] and probabilistic data association (PDA) algorithm [44].

To improve symbol detection performance, often MIMO–OFDM systems incorporate space time block codes (STBC)[45]. STBC ensure reliability for OFDM systems, by providing spatial redundancy. Most frequently used STBC are the Alamouti codes. For a 2×2 MIMO–OFDM system, implementation of Alamouti codes is simple. However as the system configuration increases, complexity of these codes also increases. For a 4 antenna system, STBC implementation is illustrated in [46]. For a system with any number of antennas, the generalized implementation of Alamouti codes is discussed in [47]. From the discussion in this section, it is clear that pilot aided channel estimation techniques for SISO–OFDM systems with LS and denoising approaches can be extended to MIMO–OFDM systems, by incorporating suitable overhead arrangements. However, for reliability of such systems, in addition to channel estimation, the symbol detection has to be improved.

5. Conclusion

The frequency domain channel estimation strategies incorporated by pilot aided OFDM systems are discussed in this paper. If pilots are arranged in comb-type, block-type or 2D-grid type fashions, interpolation is performed on the LS estimated CFR coefficients. Further, to improve the CIR estimation, denoising can be performed. A detailed survey on the available denoising strategies is presented in this paper. The survey shows that in channel environments with known KCS parameters, a variety of denoising strategies can be deployed for improved system BER performance. Of these, the threshold obtained by minimizing MSE, renders better BER performance close to that of MMSE, with the help of known three known KCS parameters, namely channel length, AWGN noise variance and number of channel taps. Hence, it can be concluded that the LS based channel estimation techniques can perform similar to the MMSE based ones, if denoising is employed. The SISO–OFDM channel estimation techniques can be extended to MIMO–OFDM systems. MIMO–OFDM systems transmit nulls in addition to pilots, to aid in channel estimation and further in sysmbol detection, which are high dimensional problems. To improve the system reliability, MIMO–OFDM systems employ STBC. A summary on available STBC and symbol detection algorithms are presented in this paper.

References

[1] K. Kusume, M. Fallgren, Updated scenarios, requirements and KPIs for 5G mobile and wireless system with recommendations for future investigations, Mobile and wireless communications Enablers for the Twenty-twenty Information Society (METIS), 2015. Document Number: ICT-317669-METIS/D1.5, Deliverable D1.5.

[2] G. Vrinda, P. Rajoo, An improved energy aware distributed unequal clustering protocol for heterogenous wireless sensor networks, in: Eng. Sci. Technol., Int. J. 19 (2016) 1050–1058.

[3] P. Ayona, A. Rajesh, Investigation on energy efficient sensor node placement in railway systems, in: Eng. Sci. Technol., Int. J. 19 (2016) 754–768.

[4] H.Q. Ngo, E.G. Larsson, T.L. Marzetta, Energy and spectral efficiency of very large multiuser MIMO systems, in: IEEE Trans. Commun. 61 (4) (2013).

[5] S. Coleri, M. Ergen, A. Puri, A. Bahai, Channel estimation techniques based on pilot arrangement in OFDM systems, IEEE Trans. Broadcast. 48 (3) (2002) 223–229.

[6] C.Y.L. Ting, An Lin, Predictive equalizer design for DVB-T system, in: IEEE Int. Symp. Circuits Syst. 2 (2005) 940–943.

[7] X. Ma, H. Kobayashi, S. Schwartz, EM-based channel estimation for OFDM, in: IEEE Pacific Rim Conference on Communications, Computers and signal Processing (PACRIM), vol. 2 (2001) 449–452.

[8] S. Jain, P. Gupta, D. Mehra, EM-MMSE based channel estimation for OFDM systems, in: IEEE International Conference on Industrial Technology (ICIT) (2006) 2598–2602.

[9] R. Prasad, C. Murthy, Bayesian learning for joint sparse OFDM channel estimation and data detection, in: IEEE Global Telecommunications Conference (GLOBECOM) (2010) 1–6.

[10] S. Wang, J. Hu, Blind channel estimation for single-input multiple-output OFDM systems: zero padding based or cyclic prefix based?, Wireless Commun Mobile Comput. 13 (2) (2013) 204–210.

[11] B. Sheng, Blind timing synchronization in OFDM systems by exploiting cyclic structure, Trans. Emerging Telecommun. Technol. 25 (2) (2014) 155–160.

[12] K.C. Hung, D.W. Lin, Pilot-aided multicarrier channel estimation via MMSE linear phase-shifted polynomial interpolation, IEEE Trans. Wireless Commun. 9 (8) (2010) 2539–2549.

[13] X.H. Jian Zhang, H. Suzuki, Phase-shifted interpolation for complex signals, in: IEEE Commun. Lett. 16 (9) (2012) 1466–1469.

[14] D. Li, F. Guo, G. Li, L. Cai, Enhanced DFT interpolation-based channel estimation for OFDM systems with virtual subcarriers, in: IEEE 63rd Vehicular Technology Conference VTC 4 (2006) 1580–1584.

[15] Y. Zhao, A. Huang, A novel channel estimation method for OFDM mobile communication systems based on pilot signals and transform-domain processing, in: IEEE Vehicular Technology Conference (VTC) (1997) 2089–2094.

[16] R.S. Cheng, Baoguo Yang, K.B. Letaief, Z. Cao, Windowed DFT based pilot-symbol-aided channel estimation for OFDM systems in multipath fading channels, in: Vehicular Technology Conference (VTC) 2 (2000) 1480–1484.

[17] J. Lei, C. Dazhong, H. Chunping, Two novel transform domain estimation methods for OFDM system and their application environment, in: Canadian Conference on Electrical and Computer Engineering, vol. 1 (2004) 377–380.

[18] A.C.D.S. Carlos Augusto Rocha, Luciano Leonel Mendes, Performance analysis of channel estimation schemes for OFDM systems, in: Proceedings of International workshop on telecommunications-IWT-2007 (2007) 32–36.

[19] A.A. Hutter, R. Hasholzner, J. Hammerschmidt, Channel estimation for mobile OFDM systems, IEEE VTS 50th Vehicular Technology Conference (VTC), vol. 1 (1999) 305–309.

[20] K. Lee, Complexity-efficient time interpolator for channel estimation in OFDM systems, Electron. Lett. 48 (5) (2012) 267–269.

[21] Pallaviram Sure, Chandra Mohan Bhuma, A pilot aided channel estimator using DFT based time interpolator for massive MIMO–OFDM systems, AEU – Int. J. Electron. Commun. 69 (1) (2015) 321–327.

[22] S. Kaiser, P. Hoeher, P. Robertson, Two-dimensional pilotsymbol-aided channel estimation by wiener filtering, in: Proc. of ICASSP Munich Germany (1997) 1845–1848.

[23] W.S.L. Xiaodai Dong, A.C.K. Soong, Linear interpolation in pilot symbol assisted channel estimation for OFDM, in: IEEE Trans. Wireless Commun. 6 (5) (2007) 1910–1920.

[24] J.J. van de Beek, O. Edfors, M. Sandell, S. Wilson, P. Ola Borjesson, On channel estimation in OFDM systems, IEEE 45th Vehicular Technology Conference, vol. 2 (1995) 815–819.

[25] H. Minn, V. Bhargava, An investigation into time-domain approach for OFDM channel estimation, IEEE Trans. Broadcast. 46 (4) (2000) 240–248.

[26] Y. Liu, S. Sezginer, Two iterative channel estimation algorithms in single-input multiple-output (SIMO) LTE systems, Trans. Emerging Telecommun. Technol. 24 (1) (2013) 59–68.

[27] F. Argenti, M. Biagini, E. Del Re, S. Morosi, Time-frequency MSE analysis of linear channel estimation methods for the LTE downlink, Trans. Emerging Telecommun. Technol. 26 (4) (2015) 704–717.

[28] M.R. Raghavendra, K. Giridhar, Improving channel estimation in OFDM systems for sparse multipath channels, IEEE Signal Process. Lett. 12 (1) (2005) 52–55.

[29] Y. Kang, K. Kim, H. Park, Efficient DFT-based channel estimation for OFDM systems on multipath channels, IET Commun. 1 (2) (2007) 197–202.

[30] J. Oliver, R. Aravind, K.M.M. Prabhu, Sparse channel estimation in OFDM systems by threshold-based pruning, IEEE Electron. Lett. 44 (13) (2008) 830–832.

[31] Y.S. Lee, H.C. Shin, H.N. Kim, Channel estimation based on a time-domain threshold for OFDM systems, IEEE Trans. Broadcast. 55 (3) (2009) 656–662.

[32] A. Alnuaimy, M. Ismail, M. Ali, Successive data schism and interpolation for channel estimation in OFDM using wavelet denoising, in: The 12th International Conference on Advanced Communication Technology (ICACT), vol. 1 (2010) 661–665.
[33] S. Rosati, G. Corazza, A. Vanelli-Coralli, OFDM channel estimation with optimal threshold-based selection of CIR samples, in: IEEE GLOBECOM (2009) 1–7.
[34] S. Rosati, G. Corazza, A. Vanelli Coralli, OFDM channel estimation based on impulse response decimation: analysis and novel algorithms, IEEE Trans. Commun. 60 (7) (2012) 1996–2008.
[35] H. Xie, G. Andrieux, Y. Wang, J.-F. Diouris, S. Feng, Efficient time domain threshold for sparse channel estimation in OFDM system, AEU – Int. J. Electron. Commun. 68 (2013) 277–281.
[36] Pallaviram Sure, Chandra Mohan Bhuma, An eigen-select denoising threshold for channel estimation in OFDM systems, Wiley International Journal of Communication Systems, 2015.
[37] Pallaviram Sure, Chandra Mohan Bhuma, Weighted-noise threshold based channel estimation for OFDM systems, Springer Sadhana J. 40 (7) (2015) 2111–2128.
[38] W. Li, X. Wang, P. Gu, D. Wang, Research on channel estimation of MIMO-OFDM system, Informatics and Management Science III, Springer, London, vol. 206 (2013) 67–73.
[39] K. Zheng, J. Su, W. Wang, Iterative DFT-based channel estimation for MIMO-OFDM systems, in: International Conference on Communications, Circuits and Systems Proceedings, vol. 2 (2006) 1081–1085.
[40] L. Dai, Z. Wang, Z. Yang, Spectrally efficient time-frequency training OFDM for mobile large-scale MIMO systems, IEEE J. Selected Areas Commun. 31 (2) (2013) 251–263.
[41] S. Mohammed, A. Zaki, A. Chockalingam, B. Rajan, High-rate space-time coded large-MIMO systems: low-complexity detection and channel estimation, IEEE J. Sel. Top. Signal Process. 3 (6) (2009) 958–974.
[42] K. Vardhan, S. Mohammed, A. Chockalingam, B. Rajan, A low-complexity detector for large MIMO systems and multicarrier CDMA systems, IEEE J. Selected Areas Commun. 26 (3) (2008) 473–485.
[43] T. Datta, N. Srinidhi, A. Chockalingam, B. Rajan, Random-restart reactive tabu search algorithm for detection in large-MIMO systems, IEEE Commun. Lett. 14 (12) (2010) 1107–1109.
[44] S. Yang, T. Lv, R. Maunder, L. Hanzo, Unified bit-based probabilistic data association aided MIMO detection for high-order QAM constellations, IEEE Trans. Vehicular Technol. 60 (3) (2011) 981–991.
[45] M.B. Breinholt, H. Jung, M.D. Zoltowski, Space-time alignment for asynchronous interference suppression in MIMO OFDM cellular communications, Wireless Commun. Mobile Comput. 4 (7) (2004) 755–771.
[46] I. Choi, J.K. Kim, H. Lee, I. Lee, Alamouti-codes based four-antenna transmission schemes with phase feedback, IEEE Commun. Lett. 13 (10) (October 2009) 749–751.
[47] P. Elia, B. A. Sethuraman, P.V. Kumar, Perfect space-time codes with minimum and non-minimum delay for any number of antennas, in: International Conference on Wireless Networks, Communications and Mobile Computing, vol. 1 (2005) 722–727.